COMPDYN 2019
7th ECCOMAS Thematic Conference on
Computational Methods in Structural Dynamics and Earthquake Engineering
M. Papadrakakis, M. Fragiadakis (eds.)
Crete, Greece, 24-26 June 2019

NONLINEAR PROGRAMMING APPROACH TO A SHEAR-DEFORMABLE HYBRID BEAM ELEMENT FOR LARGE DISPLACEMENT ANALYSIS

Charilaos M. Lyritsakis, Charalampos P. Andriotis, Konstantinos G. Papakonstantinou

The Pennsylvania State University
University Park, PA, 16802
e-mail: czl279@psu.edu
{cxa5246,kpapakon}@psu.edu

Keywords: geometrically exact beam theory, fiber elements, shear deformable beam , nonlinear programming, hybrid finite element

Abstract. *In the present work, a hybrid beam element based on exact kinematics is developed, accounting for arbitrarily large displacements and rotations, as well as shear deformable cross sections. At selected quadrature points, fiber discretization of the cross sections facilitates efficient computation of the stress resultants for any uniaxial material law. The numerical approximation is carried out through the lens of nonlinear programming, where the enengy functional of the system is treated as the objective function and the exact strain-displacement relations form the set of kinematic constraints. The only interpolated field is curvature, whereas the centerline axial and shear strains, along with the displacement measures at the element edges, are determined by enforcing compatibility through the use of any preferable constrained optimization algorithm. The solution satisfying the necessary optimality conditions is determined by the stationary point of the Lagrangian. A set of numerical examples demonstrates the accuracy and performance of the proposed element against analytical or approximate solutions available in the literature.*

1 INTRODUCTION

Problems frequently encountered by the engineering community over the last decades were concerned with structural systems whose response involved large displacements, rotations and strains on one hand, and inelastic behavior on the other. Such problems, in cases where the subject matter involved rod-like structures, necessitated the advancement of the classical Euler-Bernoulli theory, where displacements, rotations and strains were typically kept in the small range.

In the geometrically nonlinear case, the deformed geometry of the beam can be drastically different from the undeformed one, resulting in a rather involved description of beam kinematics. In general, there are two approaches in describing the kinematics of beams. The first one is the so-called continuum-based approach [1], which is employed for the derivation of the classical beam theory [2] and where all vectorial components are obtained from the three-dimensional theory of solids, with additional assumptions imposed on cross-section kinematics. The second approach, which is followed in this work, is concerned with the description of a material curve - an assemblage of material points representing the beam centroid - embedded in E^2 (or E^3 in the 3D case). The analysis of the curve by means of differential geometry of curves leads to the notion of intrinsic parameterization or one-dimensional formulation of beams, where spatial quantities can be expressed as functions of only one parameter. In the study of beams, this parameter is taken to be the arc-length of the beam. This in turn leads to the so-called arc-length parameterization of the beam with respect to a reference configuration. This approach was adopted in early works by Reissner [3, 4] and, next, Simo [5], Simo and Vu-Quoc [6] and can be traced back to Kirchhoff and his treatment of inextensible elastic rods. In these formulations, often termed as geometrically exact, the thickness of the rod is taken into consideration by attaching two vectors at each point on the material curve that would translate and rotate with the points, thus defining the properties of curvature and torsion at these points.

Approaches where strain measures are recast as primary field variables are often termed strain or deformation-based and were explored by Planinc et al. [7] for the planar case of the geometrically exact beam in order to properly account for the effect of local instabilites on the tangent stiffness matrix due to plastification, when global stability considerations are also present. It was later extended to the 2D dynamic case by Gams et al. [8] and to the three-dimensional case by Zupan and Saje [9] as a means to cope with the strain objectivity issue arising from the interpolation of the rotation vector [10]. Interpolation of strain measures is also encountered in mixed formulations, where more than one fields are interpolated and the underlying functional is augmented by additional terms to be satisfied in the weak sense [11]. Several other works with geometrically exact formulations in various settings can be found in the literature. Approaches based on mixed, hybrid, flexibility- and displacement-based considerations can be indicatively seen in [12, 13, 14, 15].

The present work is an extension of the geometrically exact hybrid formulation presented in [16] in order to account for the effect of shear deformation at the section level. As opposed to deriving the system equations from the Galerkin form after appropriate discretization, in the aforementioned work the problem is originally recast in a nonlinear programming framework, where the total potential energy functional (TPE) is augmented via Lagrange multipliers that enforce satisfaction of the exact kinematic conditions. The resulting functional is then approximated by employing a Gauss-Legendre quadrature rule, which yields the objective function to be minimized. Another interesting feature of this particular approach is that the primary variables in the element interior contributing to the elastic strain energy are the generalized strain measures of the centroid, which are sought at quadrature points. Displacement measures, namely, the translations along the coordinate axes and the rotation of the cross sections, occur only at the nodes of the element and are associated with the external work. Kinematic consistency between the rotational measures of displacement and strain is enforced by using a Lagrange interpolation scheme to approximate the curvatures over the entire element domain. We should note that quadrature points coincide with the Lagrange interpolation points. In the remainder a succinct presentation of the formulation is presented, along with numerical investigations based on benchmark nonlinear problems studied in the literature, verifying the accuracy and efficiency of the suggested approach.

2 KINEMATICS AND TOTAL POTENTIAL ENERGY

We now proceed with the derivation of the kinematic equations that serve as constraints for the optimization problem. Let us consider two dimensional Euclidian space E^2 and a fixed Cartesian coordinate system $(X_1,\ X_2)$ with unit basis vectors $\{\mathbf{E_i}\}$, $i = 1,\ 2$ and a material curve of length L which represents the centroid of the beam embedded in that space. We will assume that the beam is initially straight, aligned with the coordinate axis X_1 and in an unstressed state. We also define the arc-length parameterization of the material curve $s \in I = [0,\ L] \rightarrow \mathbf{r} \in \mathbf{R}^2$, where s is the distance of a material point on the line of centroids in the reference configuration. The position vector of any material point on the centroid in any configuration can be written as:

$$\mathbf{r}(s) = (s + u(s))\mathbf{E}_1 + w(s)\mathbf{E}_2 \tag{1}$$

where u and w are the displacements of the material point along the coordinate axes X_1 and X_2 respectively.

Beam Kinematics

According to [3] the strain-displacement relations, assuming small axial strain of the beam centroid, are:

$$u' = (1 + \epsilon)\cos\phi - \gamma\sin\phi - 1 \tag{2}$$
$$w' = (1 + \epsilon)\sin\phi + \gamma\cos\phi \tag{3}$$
$$\phi' = \kappa \tag{4}$$

where $\epsilon,\ \gamma$ and κ are the axial, shear and bending strains of the line of centroids respectively, ϕ is the tangent angle to the material curve in the current configuration and derivatives with respect to the s are denoted by $(\ )'$. Integrating (2)-(4) over I yields:

$$\begin{aligned} u(L) - u(0) &= \int_0^L (1 + \epsilon)\cos\phi - \gamma\sin\phi \, ds - L \\ w(L) - w(0) &= \int_0^L (1 + \epsilon)\sin\phi + \gamma\cos\phi \, ds \\ \phi(L) - \phi(0) &= \int_0^L \kappa \, ds \end{aligned} \tag{5}$$

The integral form of the kinematic equations in (5) is utilized to impose the constraints on the nonlinear program.

Total Potential Energy

The total potential energy functional of the beam under a set of point loads $\mathbf{P} = [\,\mathbf{P}_1 \;\; \mathbf{P}_2]^T$, with $\mathbf{P}_i$ the point loads at the element edge nodes, can be expressed in the reference configuration as:

$$\Pi(\epsilon,\ \gamma,\ \kappa,\ \mathbf{d}) = \int_0^L W(\epsilon,\ \gamma,\ \kappa)\, ds - \mathbf{P}^T\mathbf{d} \tag{6}$$

where W is the strain energy per unit length of the beam centroid. The displacement degrees of freedoms at the two edge nodes are collectively represented in vector $\mathbf{d}$ as:

$$\mathbf{d} = \begin{bmatrix} d_1 & d_2 & d_3 & d_4 & d_5 & d_6 \end{bmatrix}^T \tag{7}$$

with:

$$\begin{gathered} d_1 = u(0),\ d_2 = w(0),\ d_3 = \phi(0), \\ d_4 = u(L),\ d_5 = w(L),\ d_6 = \phi(L) \end{gathered}$$

The stress resultants on a section are associated with the strain energy as follows:

$$N = \frac{\partial W}{\partial \epsilon} \quad , \quad Q = \frac{\partial W}{\partial \gamma} \quad , \quad M = \frac{\partial W}{\partial \kappa} \tag{8}$$

The stress resultants defined in (8) can be numerically computed using appropriate fiber discretization at the cross section level. Thereby, any nonlinear constitutive law may be incorporated in beam element formulations to capture the effects of distributed elastoplastic behavior or damage [17, 18, 19].

3 NONLINEAR PROGRAMMING PROBLEM STATEMENT

In this section we formulate the equations pertaining to the description of our hybrid element as a nonlinear program.

Element Objective Function

The discrete form of the TPE in (6) is given by applying Gauss-Legendre quadrature to approximate the integral for one element:

$$f(\mathbf{x}) = \sum_{i=1}^{n} c_i W(\epsilon_i,\ \gamma_i,\ \kappa_i)\ - \mathbf{P}^T\mathbf{d} \tag{9}$$

where c_i are the weights of the quadrature, n the number of quadrature points and $\mathbf{x},\ \mathbf{d}$ and $\mathbf{y}_i$ are defined as:

$$\mathbf{x} = \begin{bmatrix} \mathbf{y}_1^T & \mathbf{y}_2^T & \dots & \mathbf{y}_n^T & \mathbf{d}^T \end{bmatrix}^T \tag{10}$$

with $\mathbf{y}_i = \begin{bmatrix} \epsilon_i & \gamma_i & \kappa_i \end{bmatrix}^T$

Element Constrains

The first set of constraints derived from the approximation of kinematic relations (5) is given as:

$$\mathbf{C}_{eq}^{A} = \begin{bmatrix} d_4 - d_1 - \sum_{i=1}^{n} c_i[(1+\epsilon_i)\cos\phi_i - \gamma_i \sin\phi_i] + L \\ d_5 - d_2 - \sum_{i=1}^{n} c_i[(1+\epsilon_i)\sin\phi_i + \gamma_i \cos\phi_i] \\ d_6 - d_3 - \sum_{i=1}^{n} c_i \kappa_i \end{bmatrix} = \mathbf{0} \tag{11}$$

In accordance with [16] we then interpolate the curvature field with Lagrange polynomials in order to obtain the rotations ϕ_i at the quadrature points:

$$\phi_i = d_3 + \sum_{j=1}^{n} \Theta_{ij} \kappa_j \tag{12}$$

$$\boldsymbol{\Theta} = L \begin{bmatrix} \xi_1 & \frac{\xi_1^2}{2} & \dots & \frac{\xi_1^n}{n} \\ \vdots & \vdots & \ddots & \vdots \\ \xi_n & \frac{\xi_n^2}{2} & \dots & \frac{\xi_n^n}{n} \end{bmatrix} \mathbf{G}^{-1}, \quad \mathbf{G} = \begin{bmatrix} 1 & \xi_1 & \dots & \xi_1^{n-1} \\ \vdots & \vdots & \ddots & \vdots \\ 1 & \xi_n & \dots & \xi_n^{n-1} \end{bmatrix} \tag{13}$$

where $\xi = \frac{x}{L}$ and $\mathbf{G}$ is the Vandermonde matrix.

Notice that the first two equations of (11) are *nonlinear equality* constraints, while the third, along with the n equations of (12) are *linear equality* constraints. It is convenient to recast all constraints in one vector as follows:

$$\mathbf{C}_{eq} = \begin{bmatrix} \mathbf{C}_{eq}^{A} \\ \\ \mathbf{C}_{eq}^{B} \end{bmatrix} = \mathbf{0} \tag{14}$$

where

$$\mathbf{C}_{eq}^{B} = \begin{bmatrix} \phi_1 - d_3 - \sum_{j=1}^{n} \Theta_{1j}\kappa_j \\ \vdots \\ \phi_n - d_3 - \sum_{j=1}^{n} \Theta_{nj}\kappa_j \end{bmatrix} \tag{15}$$

Element Lagrangian Function

We now introduce a vector $\boldsymbol{\lambda}$ of the Lagrange multipliers and augment the TPE (6), constructing the Lagrangian of the optimization problem as:

$$f(\mathbf{x},\ \boldsymbol{\lambda}) = \sum_{i=1}^{n} c_i W(\epsilon_i,\ \gamma_i,\ \kappa_i)\ - \mathbf{P}^T\mathbf{d} + \boldsymbol{\lambda}^T \mathbf{C}_{eq} \tag{16}$$

Stationary points are provided by satisfying Karush-Kuhn-Tucker [20] optimality conditions for the Lagrangian function of (16).

4 NUMERICAL EXAMPLES

In the following examples we examine the performance of the proposed formulation and compare it with other well-known works in the literature. We first explore the accuracy when the shear stiffness is reduced and then we test against different loading cases. For each example, only one element with five quadrature points is used.

Table 1: Cantilever with constant transverse load at free end.

	w			u		
GA_s	Numerical	Analytical	Present	Numerical	Analytical	Present
$5 \cdot 10^{20}$	0.30172077	0.301720774	0.30172432	0.05643324	0.056433236	0.05643126
$5 \cdot 10^{2}$	0.31781387	0.317813874	0.31781567	0.06131566	0.061315658	0.06131317
$5 \cdot 10^{1}$	0.46541330	0.465413303	0.46541543	0.10328492	0.103284917	0.10328294
$1 \cdot 10^{2}$	1.16709588	1.167095878	1.16709542	0.25213661	0.252136606	0.25213357
$5 \cdot 10^{0}$	2.10408747	2.104087473	2.10409063	0.37612140	0.376121399	0.37612451

Problem data: $EA = 10^{21},\ EI = 10,\ L = 1$. Numerical data in [21], analytical in [22].

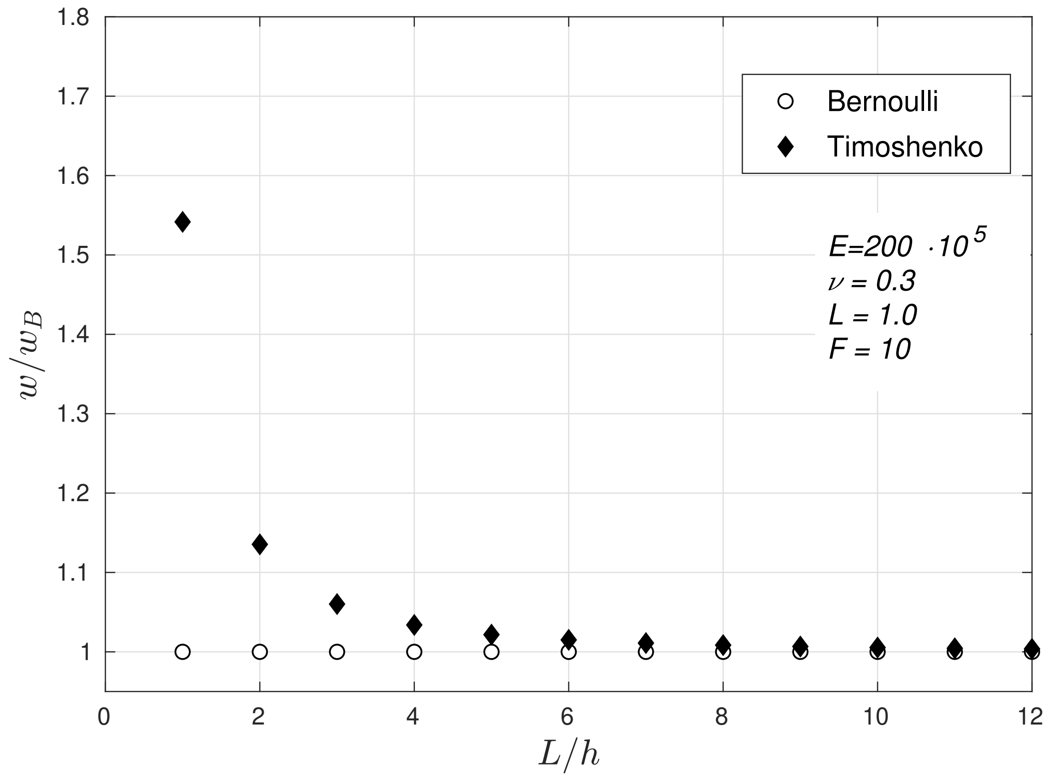

Figure 1: Timoshenko compared to Bernoulli solutions for different levels of slenderness.

Example 1 - Effect of shear deformation in cantilever deflection

In this example we explore the effect of shear flexibility on the tip deflection of a cantilever. A constant point transverse force $P = 10$ units is applied at the free end and, then, several analyses are performed by varying the shear stiffness coefficient, GA_s. Numerical and analytical results obtained by Batista in [21] and [22], respectively, are compared with the present formulation and are illustrated in Table 1.

Fig. 1 demonstrates the effect shear deformations have when not neglected, compared to the Bernoulli solutions, by varying the ratio L/h, with h being the height of the cross section and L the length of the beam. The applied load is F, ν is the Poisson's ratio and w_B is the deflection when shear flexibility is neglected. As can be seen from the results, when $L = 2h$, transverse displacements due to shear deformation are increased by rougly 13%.

Example 2 - Cantilever with transverse point load at its tip

This problem has been analyzed in [23, 24], whereas Mattiasson [25] provided solutions by solving the elliptic integrals of the problem of large deflections of beams. Moreover, the problem was also examined in [26] using a co-rotational transformation for the Timoshenko beam, whereas Nanakorn [27] used 3 elements and a total tagrangian formulation.

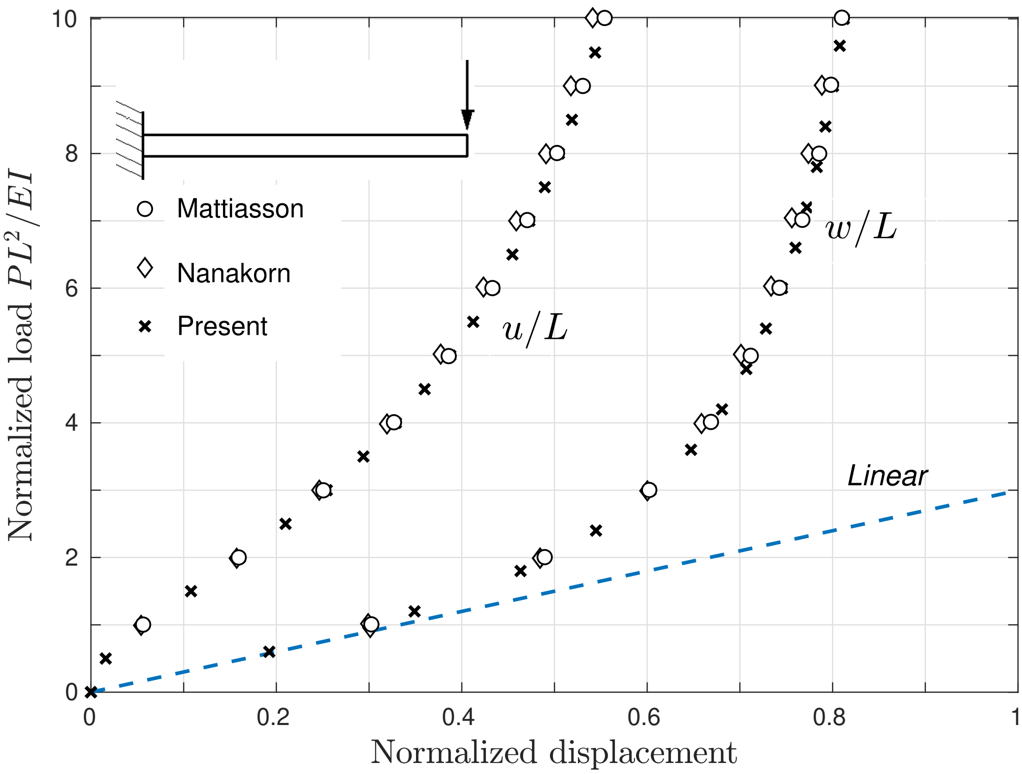

Figure 2: Cantilever with point transverse load at its free end.

Table 2: Cantilever with transverse load at its free end.

	w/L		u/L	
PL^2/EI	Mattiasson	Present	Mattiasson	Present
2.0	0.49346	0.49347	0.16064	0.16063
4.0	0.66996	0.67001	0.32894	0.32892
6.0	0.74457	0.74465	0.43459	0.43457
8.0	0.78498	0.78509	0.50483	0.50481
10.0	0.81061	0.81073	0.55500	0.55498

Problem data: $EI = 1000$ lb/in^2, $L = 100$in, $P = 1$lb, $N = 20$ steps.
Results in Mattiasson [25].

Figure 2 illustrates the performance of the element when compared against the analytical and numerical solutions - mentioned above - and Table 2 demonstrates the accuracy up to six decimal points when compared to the analytical solutions for a sample of loading levels. The dotted line indicates the linear response.

Example 3 - Cantilever with point moment at its free end

This example tests the capabilities of our developed model capturing the response of an inextensional beam subjected to a point moment, forcing a curl into a complete circle. As mentioned previously, in all examples we only used one element with five quadrature points for our analysis. Bathe and Bolourchi [28] using five and twenty elements and an updated lagrangian procedure showed accuracy up to 90 degrees. In subsequent works, Simo & Vu-Quoc [6] (five elements), Rankin & Brogan [29] (ten elements) and Crisfield [30] (five elements) duplicated the exact solution. In the second and third works a corotational formulation was employed. The mechanical and geometric properties for this problem are $I = 0.01042\text{in}^4$, $L = 100\text{in}$, $A = 0.5\text{in}^2$, $E = 1.2 \times 10^4\text{psi}$.

In Fig. 3 our solution is compared with the one using twenty elements. As mentioned earlier, with the element proposed by Bathe & Bolourchi [28], which is based on large-displacement and large-rotation assumptions, the response starts to diverge from the exact solution at an angle of 90 degrees rotation, irrespectively of the mesh density. Our proposed formulation is instead able to capture the response for the whole loading scenario (360 degrees), as can be seen from the line that represents the normalized displacement $\phi/2\pi$.

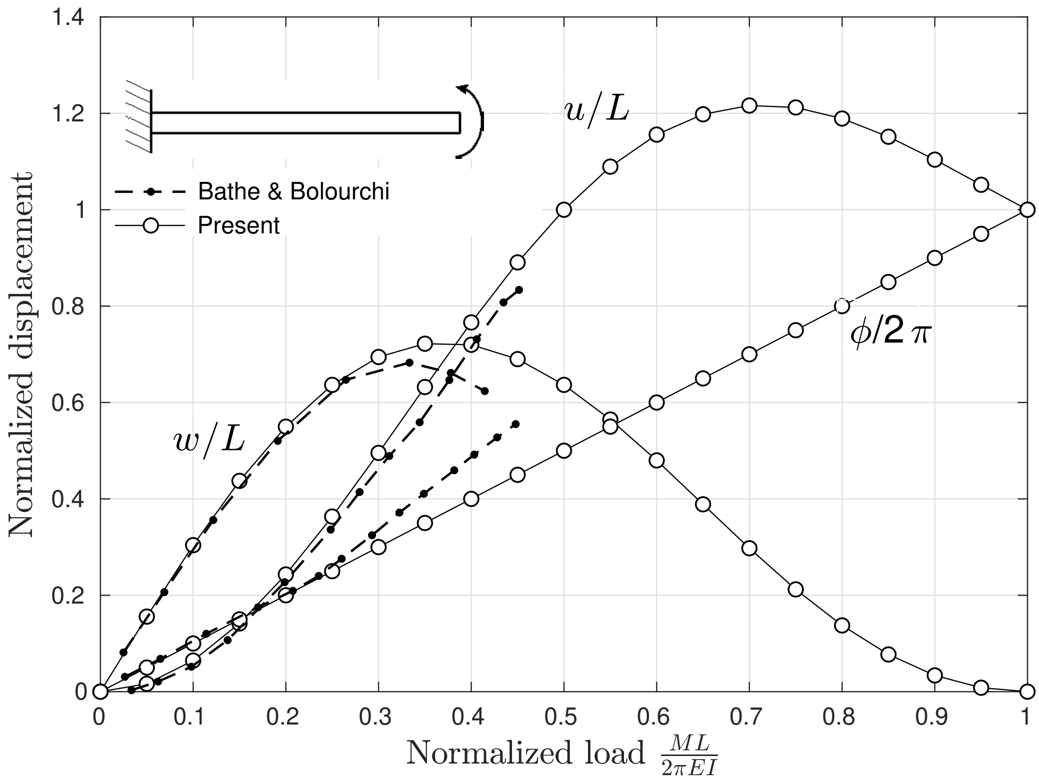

Figure 3: Cantilever with point moment at its free end.

Example 4 - Cantilever beam with eccentric compressive point load

We consider a cantilever beam of length $L = 100$, cross section thickness $b = 1$ and elastic modulus $E = 12$, with the load parameter $\lambda = P/P_{cr}$ is increased up to 4.0. The critical load for the cantilever is $P_{cr} = 0.25\pi^2 EI/L^2$. Wood & Zienkiewicz [31] used five continuum-based elements that allow for shear deformation and employed a total Lagrangian formulation. The results are illustrated in Fig. 4. Analytical solutions to the problem, provided in [23, 32] where it is assumed no axial or shear deformation occurs, show negligible discrepancy compared to the ones proposed here and in [31]. It should be noted that the eccentricity is $\epsilon = b/2$. The configurations for each load step for Examples 2,3 and 4 are depicted in Fig. 5, from left to right.

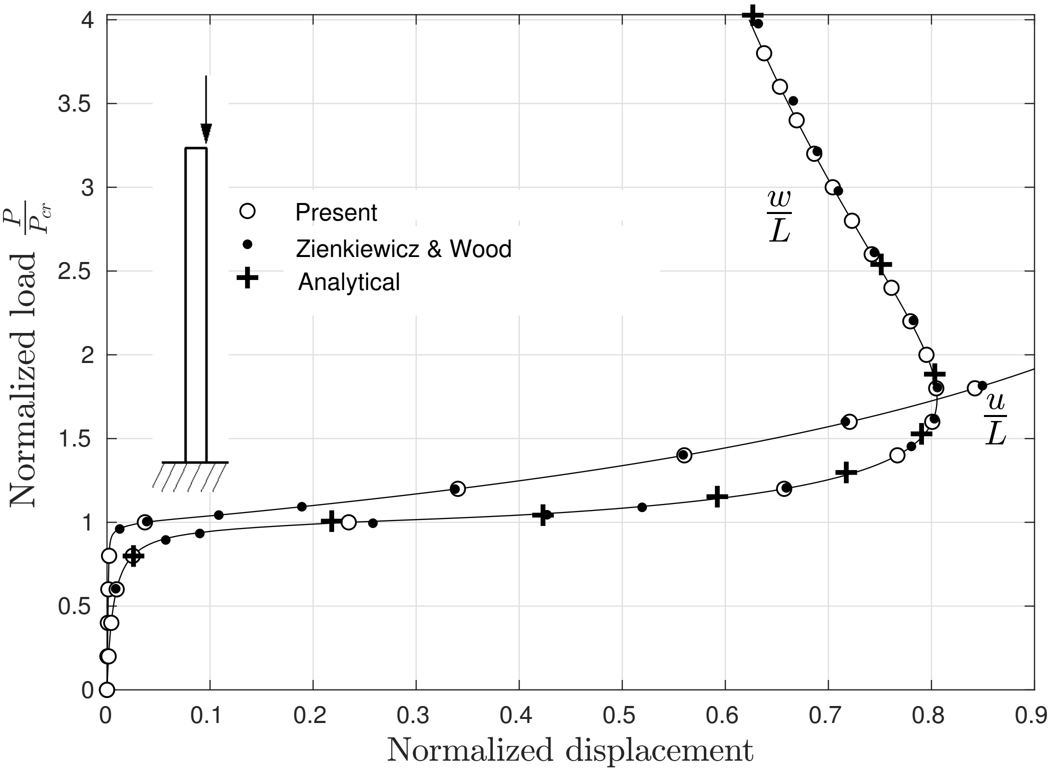

Figure 4: Cantilever with eccentric axial load at its free end.

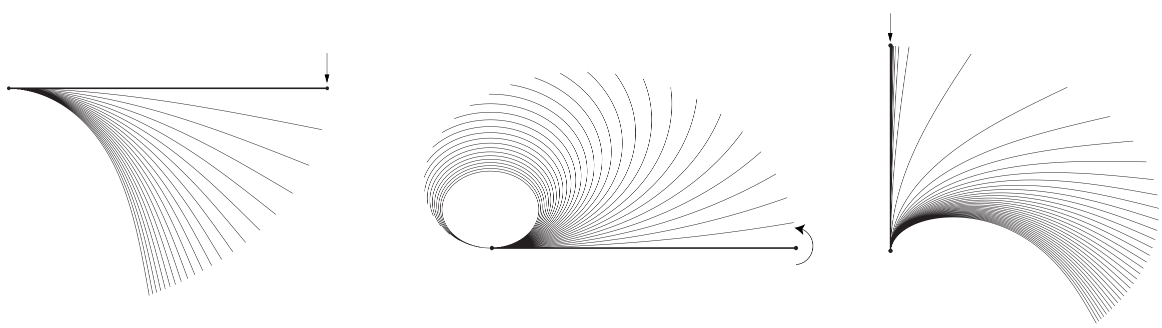

Figure 5: Configurations at each step for examples 2, 3 and 4 (left to right).

5 CONCLUSIONS

An extension to the geometrically exact hybrid element derived in [16] is presented herein that accounts for shear deformations. The system of equilibrium equations is originally derived within a nonlinear programming framework, where the total potential energy functional is discretized and then augmented by the exact kinematic constraints of the physical problem, also in discretized form, and solved by determining the stationary point of the Lagrangian. The suggested nonlinear programming hybrid formulation is capable of capturing the response of the benchmark problems with accuracy, using only one element, which is a desirable feature for framed structure applications. Ongoing work explores a variety of different approaches as far as the optimization algorithms are concerned, which is something the proposed formulation supports and enables, the extension of the material yield rule to account for the interaction of shear and axial stresses, as well as the extension to spatial and dynamic formulations.

Acknowledgements

This material is based upon work supported by the National Science Foundation under Grant No. 1634575. The authors gratefully acknowledge this support.

REFERENCES

[1] T. Belytschko, L. Schwer, and M.J. Klein. Large displacement, transient analysis of space frames. *International Journal for Numerical Methods in Engineering*, **11**(1):65–84, 1977.

[2] T.J.R. Hughes. *The finite element method: linear static and dynamic finite element analysis*. Dover, 2000.

[3] E. Reissner. On one-dimensional finite-strain beam theory: The plane problem. *Zeitschrift für Angewandte Mathematik und Physik ZAMP*, **23**(5):795–804, 1972.

[4] E. Reissner. On one-dimensional large-displacement finite-strain beam theory. *Studies in applied mathematics*, **52**(2):87–95, 1973.

[5] J.C. Simo. A finite strain beam formulation. The three-dimensional dynamic problem. Part I. *Computer Methods in Applied Mechanics and Engineering*, **49**(1):55–70, 1985.

[6] J.C. Simo and L. Vu-Quoc. A three-dimensional finite-strain rod model. Part II: Computational aspects. *Computer Methods in Applied Mechanics and Engineering*, 58(1):79–116, 1986.

[7] I. Planinc, M. Saje, and B. Cas. On the local stability condition in the planar beam finite element. *Structural Engineering and Mechanics*, **12**(5):507–526, 2001.

[8] M. Gams, M. Saje, S. Srpčič, and I. Planinc. Finite element dynamic analysis of geometrically exact planar beams. *Computers & Structures*, **85**(17-18):1409–1419, 2007.

[9] D. Zupan and M. Saje. Finite-element formulation of geometrically exact three-dimensional beam theories based on interpolation of strain measures. *Computer Methods in Applied Mechanics and Engineering*, **192**(49-50):5209–5248, 2003.

[10] M.A. Crisfield and G. Jelenić. Objectivity of strain measures in the geometrically exact three-dimensional beam theory and its finite-element implementation. *Proceedings of the Royal Society of London. Series A: Mathematical, Physical and Engineering Sciences*, **455**(1983):1125–1147, 1999.

[11] C.A. Felippa. A survey of parametrized variational principles and applications to computational mechanics. *Computer Methods in Applied Mechanics and Engineering*, **113**(1-2):109–139, 1994.

[12] M.V. Sivaselvan and A.M. Reinhorn. Collapse analysis: large inelastic deformations analysis of planar frames. *Journal of Structural Engineering*, **128**(12):1575–1583, 2002.

[13] H.A.F.A. Santos, P.M. Pimenta, and J.P.M. Almeida. A hybrid-mixed finite element formulation for the geometrically exact analysis of three-dimensional framed structures. *Computational Mechanics*, **48**(5):591, 2011.

[14] N.D. Oliveto and M.V. Sivaselvan. 3D finite-deformation beam model with viscous damping: Computational aspects and applications. *Journal of Engineering Mechanics*, **141**(1):04014103, 2014.

[15] M. Salehi and P. Sideris. A finite-strain gradient-inelastic beam theory and a corresponding force-based frame element formulation. *International Journal for Numerical Methods in Engineering*, **116**(6):380–411, 2018.

[16] C.P. Andriotis, K.G. Papakonstantinou, and V.K. Koumousis. Nonlinear programming hybrid beam-column element formulation for large-displacement elastic and inelastic analysis. *Journal of Engineering Mechanics*, **144**(10):04018096, 2018.

[17] E. Spacone, F.C. Filippou, and F.F. Taucer. Fibre beam–column model for non-linear analysis of R/C frames: Part I. Formulation. *Earthquake Engineering & Structural Dynamics*, **25**(7):711–725, 1996.

[18] P. Uriz, F.C. Filippou, and S.A. Mahin. Model for cyclic inelastic buckling of steel braces. *Journal of Structural Engineering*, **134**(4):619–628, 2008.

[19] C. Andriotis, I. Gkimousis, and V. Koumousis. Modeling reinforced concrete structures using smooth plasticity and damage models. *Journal of Structural Engineering*, **142**(2):04015105, 2015.

[20] J. Nocedal and S. Wright. *Numerical Optimization*. Springer Science & Business Media, 2006.

[21] M. Batista and F. Kosel. Cantilever beam equilibrium configurations. *International Journal of Solids and Structures*, **42**(16-17):4663–4672, 2005.

[22] M. Batista. A closed-form solution for Reissner planar finite-strain beam using Jacobi elliptic functions. *International Journal of Solids and Structures*, **87**:153–166, 2016.

[23] R. Frisch-Fay. *Flexible bars*. Butterworths, 1962.

[24] K.E. Bisshopp and D.C. Drucker. Large deflection of cantilever beams. *Quarterly of Applied Mathematics*, **3**(3):272–275, 1945.

[25] K. Mattiasson. Numerical results from large deflection beam and frame problems analysed by means of elliptic integrals. *International Journal for Numerical Methods in Engineering*, **17**(1):145–153, 1981.

[26] N.D. Kien. A Timoshenko beam element for large displacement analysis of planar beams and frames. *International Journal of Structural Stability and Dynamics*, **12**(06):1250048, 2012.

[27] P. Nanakorn and L.N. Vu. A 2D field-consistent beam element for large displacement analysis using the total Lagrangian formulation. *Finite Elements in Analysis and Design*, **42**(14-15):1240–1247, 2006.

[28] Klaus-Jürgen Bathe and S. Bolourchi. Large displacement analysis of three-dimensional beam structures. *International Journal for Numerical Methods in Engineering*, **14**(7):961–986, 1979.

[29] C.C. Rankin and F.A. Brogan. An element independent corotational procedure for the treatment of large rotations. *Journal of Pressure Vessel Technology*, **108**(2):165–174, 1986.

[30] M.A. Crisfield. A consistent co-rotational formulation for non-linear, three-dimensional, beam-elements. *Computer Methods in Applied Mechanics and Engineering*, **81**(2):131–150, 1990.

[31] R.D. Wood and O.C. Zienkiewicz. Geometrically nonlinear finite element analysis of beams, frames, arches and axisymmetric shells. *Computers & Structures*, **7**(6):725–735, 1977.

[32] S.P. Timoshenko and J.M. Gere. *Theory of elastic stability*. Dover, 2009.